Kv2.1 Clustering Contributes to Insulin Exocytosis and Rescues Human β-Cell Dysfunction

Jianyang Fu,[1,2] Xiaoqing Dai,[1,2] Gregory Plummer,[1,2] Kunimasa Suzuki,[1,2] Austin Bautista,[1,2] John M. Githaka,[3] Laura Senior,[1,2] Mette Jensen,[4] Dafna Greitzer-Antes,[5] Jocelyn E. Manning Fox,[1,2] Herbert Y. Gaisano,[5] Christopher B. Newgard,[4] Nicolas Touret,[3] and Patrick E. MacDonald[1,2]

Diabetes 2017;66:1890–1900 | https://doi.org/10.2337/db16-1170

Insulin exocytosis is regulated by ion channels that control excitability and Ca^{2+} influx. Channels also play an increasingly appreciated role in microdomain structure. In this study, we examine the mechanism by which the voltage-dependent K^+ (Kv) channel Kv2.1 (*KCNB1*) facilitates depolarization-induced exocytosis in INS 832/13 cells and β-cells from human donors with and without type 2 diabetes (T2D). We find that Kv2.1, but not Kv2.2 (*KCNB2*), forms clusters of 6–12 tetrameric channels at the plasma membrane and facilitates insulin exocytosis. Knockdown of Kv2.1 expression reduces secretory granule targeting to the plasma membrane. Expression of the full-length channel (Kv2.1-wild-type) supports the glucose-dependent recruitment of secretory granules. However, a truncated channel (Kv2.1-ΔC318) that retains electrical function and syntaxin 1A binding, but lacks the ability to form clusters, does not enhance granule recruitment or exocytosis. Expression of *KCNB1* appears reduced in T2D islets, and further knockdown of *KCNB1* does not inhibit Kv current in T2D β-cells. Upregulation of Kv2.1-wild-type, but not Kv2.1-ΔC318, rescues the exocytotic phenotype in T2D β-cells and increases insulin secretion from T2D islets. Thus, the ability of Kv2.1 to directly facilitate insulin exocytosis depends on channel clustering. Loss of this structural role for the channel might contribute to impaired insulin secretion in diabetes.

The regulated exocytosis of insulin containing secretory granules is critical for glucose homeostasis, and impaired insulin secretion from β-cells of the pancreatic islets of Langerhans is a key factor in the development of type 2 diabetes (T2D) (1). In response to elevated plasma glucose, the mitochondrial generation of ATP within β-cells results in closure of ATP-dependent K^+ (K_{ATP}) channels, action potential firing, and activation of voltage-dependent Ca^{2+} channels; the subsequent entry of Ca^{2+} triggers exocytosis of insulin containing dense-core vesicles (reviewed in Ref. 2).

The repolarization of β-cell action potentials is mediated by delayed rectifier K^+ channels, and in rodents, this is largely mediated by the voltage-dependent K^+ (Kv) channel isoform Kv2.1 (3,4). However, even though human β-cells express abundant Kv2.1 channels encoded by *KCNB1* (5–8), inhibition of these (and the related Kv2.2) has little effect on human β-cell electrical function and variable effects on insulin secretion from human islets (6,9). Additionally, control of Kv2.2 expression may also contribute to the regulation of insulin secretion (10), and recent transcriptomic analysis of purified β-cells suggests an ~10-fold higher expression of the Kv2.2-encoding gene *KCNB2* versus *KCNB1* (11). Thus, the role for Kv2.1 channels in insulin secretion, particularly in humans, remains unclear.

Interestingly, Kv2.1 may play a direct role in the exocytotic process, independent of its pore function, through an interaction with syntaxin 1A at the channel C terminus (12). Indeed, this is true in both rodent and human β-cells, in which we demonstrated that disruption of the Kv2.1–syntaxin 1A interaction impairs depolarization-induced exocytosis and insulin secretion (7). Tetrameric Kv2.1 channels target to distinct membrane microdomains or clusters, and this requires a C-terminal region of the channel (13–15) that

[1]Alberta Diabetes Institute, University of Alberta, Edmonton, Alberta, Canada
[2]Department of Pharmacology, University of Alberta, Edmonton, Alberta, Canada
[3]Department of Biochemistry, University of Alberta, Edmonton, Alberta, Canada
[4]Sarah W. Stedman Nutrition and Metabolism Center and Duke Molecular Physiology Institute, Departments of Pharmacology & Cancer Biology and Medicine, Duke University, Durham, NC
[5]Departments of Medicine and Physiology, University of Toronto, Toronto, Ontario, Canada
Corresponding author: Patrick E. MacDonald, pmacdonald@ualberta.ca.

Received 26 September 2016 and accepted 15 April 2017.
This article contains Supplementary Data online at http://diabetes.diabetesjournals.org/lookup/suppl/doi:10.2337/db16-1170/-/DC1.

does not overlap with the syntaxin-binding domain. A physiological role for Kv2.1 channel clusters, which may be electrically silent (16) because of increased channel density (17), is not readily apparent, although they likely play a role in the exocytosis of GLUT4-containing vesicles (18) and appear to define regions of plasma membrane association with the cortical endoplasmic reticulum (19).

In this study, we have examined the role for Kv2 channels as facilitators of insulin exocytosis in pancreatic β-cells from human donors with and without T2D. We find that Kv2.1 and 2.2 both contribute to the delayed outward K^+ current, but that only Kv2.1 facilitates insulin exocytosis. Expression of *KCNB1* and *KCNB2* and the contribution of these channels to outward K^+ currents are reduced in islets from donors with T2D, in which upregulation of full-length Kv2.1 restores exocytotic function and increases insulin secretion. Mechanistically, tetrameric Kv2.1 channels cluster at the plasma membrane, and these are required for efficient insulin granule recruitment independent of the channel's ability to conduct K^+ or bind syntaxin 1A. Thus, we demonstrate an important structural role for Kv2.1 at the plasma membrane of pancreatic β-cells, the loss of which may contribute to impaired insulin secretion in T2D.

RESEARCH DESIGN AND METHODS

Cells and Tissues

Human embryonic kidney (HEK) 293 cells were cultured in DMEM with 20 mmol/L glucose, 10% FBS, 100 units/mL penicillin, and 100 mg/mL streptomycin at 37°C and 5% CO_2. The glucose-responsive INS 832/13 insulinoma cell line (20) was cultured in RPMI 1640 with 11.1 mmol/L glucose, 10% FBS, 10 mmol/L HEPES, 0.29 mg/mL L-glutamine, 1 mmol/L sodium pyruvate, 50 μmol/L 2-mercaptoethanol (2-ME), and 100 U/mL penicillin/streptomycin. Human islets from the Clinical Islet Laboratory at the University of Alberta and the Alberta Diabetes Institute IsletCore (21) were cultured in low-glucose (5.5 mmol/L) DMEM with L-glutamine, 110 mg/L sodium pyruvate, 10% FBS, and 100 U/mL penicillin/streptomycin. Islets from 40 donors without diabetes (ND) and 15 donors with T2D contributed to this work (Supplementary Tables 1–3). All human islet studies were approved by the Human Research Ethics Board (Pro00001754) at the University of Alberta, and all families of organ donors provided written informed consent.

Molecular Biology

Knockdown of *KCNB1* or *KCNB2* expression in human cells was carried out using a mixture of four small interfering RNA (siRNA) duplexes (Qiagen, Toronto, Ontario, Canada), in which each recognizes different regions of the target gene. Transfected cells were identified by cotransfection with an Alexa Fluor 488–tagged duplex (catalog number 1027292; Qiagen). Adenoviral short hairpin RNA constructs to knock down rat *Kcnb1* or *Kcnb2* in INS 832/13 cells are described (10). Knockdown of *KCNB1* or *KCNB2* in human islets was confirmed by quantitative PCR using TaqMan expression assays (Applied Biosystems/Thermo Fisher Scientific, Waltham, MA). The cDNA encoding wild-type (WT) rat Kv2.1 or the truncated Kv2.1-ΔC318 (Kv2.1 Glu536_Ile853 del) was amplified by PCR using a pCDNA3-Kv2.1 plasmid as a template and inserted between the *Bsr*GI and *Xho*I site of Cherry-LacRep plasmid (22) (from Mirek Dundr, Rosalind Franklin University of Medicine and Science; Addgene plasmid 18985) by Gibson Assembly to make pmCherry-Kv2.1-WT and pmCherry-Kv2.1-ΔC318.

To generate a photoactivatable (PA) construct for photoactivated localization microscopy (PALM), the mCherry cDNA in pmCherry-Kv2.1-WT was replaced with PAmCherry cDNA amplified by PCR from pPAmCherry1-C1 (23) (from Vladislav Verkhusha, Albert Einstein College of Medicine; Addgene plasmid 31929) and inserted between *Nhe*I and *Bsr*GI of the pmCherry-Kv2.1-WT plasmid. To generate Myc-tagged constructs, the cDNA-encoding 5xMyc was inserted between *Nhe*I and *Bsr*GI sites of the pmCherry-Kv2.1 WT and pmCherry-Kv2.1-ΔC318 expression vector by Gibson Assembly. The Kv2.1 pore mutant ($Kv2.1^{W365C/Y380T}$) was described previously (7,12) and used to create the GFP-coexpressing adenovirus Ad-$Kv2.1^{W365C/Y380T}$ (Welgen Inc., Woster, MA). Adenovirus expressing GFP alone was a control (Ad-GFP; Welgen Inc.).

Electrophysiology and Insulin Secretion

Patch-clamp measurement of Kv currents and exocytosis in single INS 832/13 or human β-cells, identified by positive insulin immunostaining following the experiment, was performed at 32–35°C as described (7). Insulin secretion was measured, 48 h following adenoviral infection, in human islets by perifusion at 37°C in Krebs-Ringer buffer: 115 mmol NaCl, 5 mmol KCl, 24 mmol $NaHCO_3$, 2.5 mmol $CaCl_2$, 1 mmol $MgCl_2$, 10 mmol HEPES, and 0.1% BSA (pH 7.4). Twenty islets per lane were perifused (0.25 mL/min) with 1 mmol/L glucose Krebs-Ringer buffer for 24 min and then with the indicated condition. Samples were collected over 2-min intervals. Islets were lysed in acid/ethanol buffer (1.5% concentrated HCl, 23.5% acetic acid, and 75% ethanol) for total insulin content. Samples were assayed using the Insulin Detection Kit (Meso Scale Discovery).

Total Internal Reflection Fluorescence and PALM Imaging

Imaging was performed on fixed cells, except for live-cell data in Fig. 8*G–I*, 36–48 h after transduction with mCherry-tagged channel constructs and Venus- or EGFP-tagged neuropeptide Y (NPY) to mark secretory granules or following immunostaining for Kv2.1 and insulin with antibodies diluted in 1:1,000 monoclonal mouse anti-Kv2.1 (University of California Davis/National Institutes of Health NeuroMab Antibodies, Davis, CA) and 1:1,000 polyclonal guinea pig anti-insulin (Dako Canada, Burlington, Ontario, Canada) diluted in 5% goat serum or 2% donkey serum. Detection was with Alexa Fluor 488– or 594–conjugated secondary antibodies (Molecular Probes, Eugene, OR) diluted 1:2,000 as above.

All total internal reflection fluorescence (TIRF) imaging used a Cell-TIRF motorized system (IX83P2ZF; Olympus

Canada) with a 100×/1.49 NA TIRFM objective, a Photometrics Evolve 512 camera (Photometrics), and Metamorph Imaging software (Molecular Devices). Stimulation was at 491 nm (LAS-491–50) and 561 nm (LAS-561–50; Olympus) with a quad filter passing through a major dichroic and band pass filter (405/488/561/640; Chroma Technology, Bellows Falls, VT). Penetration depth was set to 105 nm, calculated using the existing angle of the laser and assuming a refractive index of 1.37. Emission was collected through bandpass filters of 525/25 nm and 605/26 nm for excitations of 488 and 561 nm, respectively. Images were acquired sequentially with single-laser excitation to minimize potential bleed-through. Object-based colocalization was performed using Imaris Scientific 3D/4D Image Processing software (Bitplane, Zurich, Switzerland, v7.3.2) on top hat–filtered and background-subtracted images. A Gaussian filter assuming initial spot diameter of 0.3 μm was used to initially identify spots, and region growing was applied to ensure capture of clusters with differing sizes. The "Colocalize Spots" function, calculated by MATLAB (r2013; MathWorks), was run with a center-to-center threshold value of 0.3 μm, which is <2 pixels and represents the minimum resolvable distance to distinguish two objects in our system. Live-cell acquisition was 5 Hz with a 200-ms exposure at 35°C. Before acquisition, cells were preincubated (30 min) in a bath containing 138 mmol NaCl, 5.6 mmol KCl, 1.2 mmol $MgCl_2$, 2.6 mmol $CaCl_2$, 5 mmol $NaHCO_3$, 1 mmol glucose, and 5 mmol HEPES (pH 7.4 with NaOH) and then exposed to 5 mmol/L glucose upon recording. Fusion events, indicated by abrupt brightening (ratio of peak fluorescence to background >1.3) and then disappearance of NPY-EGFP fluorescence, were selected and analyzed with computer-assisted analysis software (24) and normalized to membrane area.

For PALM imaging (25), cells were fixed on ice with 3% glutaraldehyde for 10 min followed by quenching with 0.1% sodium borohydride to minimize autofluorescence by quenching free aldehyde groups. A low-power (20 μW) 405-nm UV-laser (Spectral Applied Research, Richmond Hill, Canada) was used to photo-activate PAmCherry, of which the signal was acquired using a 605/20-nm bandpass filter after excitation with 1 mW of a 561-nm laser (Spectral Applied Research) at 100-ms exposure time until all molecules were photo-bleached. Acquisition was with a 100× (1.45 NA) oil objective, a Hamamatsu EM-CDD camera (ImageEM91013; Hamamatsu), and Volocity software (PerkinElmer). To identify clusters, Spatial Pattern Analysis was computed as previously described with Gaussian-mixture model fitting (26–28). To avoid potential molecule overcounting from emission by the same molecules, multiappearance localizations were eliminated (26). Cluster spatial maps were generated by calculation of second-order neighborhood local density value Li(r) for each coordinate. To obtain cluster properties, a robust and unbiased thresholding approach was applied to segment the local density spatial maps and identify regions from which cluster properties could be computed (26,29).

Extracellular Cross-linking and Immunoprecipitation

Cross-linking was performed with the membrane-impermeable thiol-cleavable cross-linker 3,3′dithiobis (sulfosuccinimidyl-propionate) (DTSSP; Thermo Fisher Scientific). INS 832/13 or HEK 293 cells (10^7 cells/reaction) were incubated with 25 mmol/L DTSSP in distilled water at room temperature for 30 min. After the incubation, cells were washed two times with PBS, and remaining DTSSP was blocked by 15-min incubation with 50 mmol/L stop solution (1 mol/L Tris [pH 7.5]). Cell lysates were harvested in RIPA buffer, separated using SDS-PAGE, transferred to polyvinylidene difluoride membrane, and probed with mouse polyclonal anti-Myc antibody (1:2,000; Merck Millipore, Billerica, MA), mouse anti–β-tubulin antibody (1:2,000; Sigma-Aldrich, St. Louis, MO), or mouse anti-Kv2.1 (1:1,000 in 5% BSA; University of California Davis/National Institutes of Health NeuroMab Antibodies). Immunoprecipitation using syntaxin 1A antibody (4E209; sc-73098) from Santa Cruz Biotechnology was as described before (7). Densitometry was performed using ImageJ software (National Institutes of Health; http://imagej.nih.gov/ij/).

Statistical Analysis

Data analysis was performed using FitMaster (HEKA Electronik), Origin Lab (v7.0), and Prism (v6.0c; GraphPad Software). All data are shown as means ± SEM. Statistical outliers were identified by an unbiased robust regression followed by outlier identification (ROUT) test (30). Comparison of multiple groups was by ANOVA and Bonferroni posttest. When comparing two means only, data were analyzed by the two-tailed Student *t* test. A *P* value <0.05 was considered significant.

RESULTS

Kv2.1 and 2.2 Mediate Outward K^+ Currents in Human β-Cells, but Only Kv2.1 Facilitates Exocytosis

Pharmacological inhibitors of Kv2 channels and dominant-negative strategies, which are not selective for Kv2.1 versus Kv2.2 enhance electrical excitability, prolong the action potential duration, increase intracellular Ca^{2+} responses, and enhance insulin secretion from rodent islets (3,31). Although their role in insulin secretion from human islets is debated (6,9), and we also find no effect of the Kv2 inhibitor stromatoxin on insulin secretion from human islets (Supplementary Fig. *1A*), it is clear that human pancreatic β-cells express robust Kv2-mediated currents (5–8). Although often interpreted as an important role for Kv2.1, recent work in insulinoma cells suggests a key contribution of Kv2.2 (10), and transcriptomic data demonstrate that purified β-cells express more *KCNB2* than *KCNB1* (11). Indeed, we find that in human islets, *KCNB2* expression is 8.7 ± 2.0-fold higher than that of *KCNB1* (Fig. 1*A*). Selective knockdown of *KCNB1* or *KCNB2* in human β-cells (Fig. 1*B*) demonstrates that each isoform contributes to the outward delayed rectifier current in these cells (Fig. 1*C* and *D*). However, knockdown of *KCNB1*, but not *KCNB2*, impairs depolarization-induced exocytosis in human β-cells (Fig. 1*E*

and *F*), which is consistent with the divergent C-terminal homology and an inability of Kv2.2 to bind the syntaxin 1A/SNAP-25 complex (32). Similar results were obtained upon knockdown of *Kcnb1* and *Kcnb2* in INS 832/13 insulinoma cells (Supplementary Fig. 2).

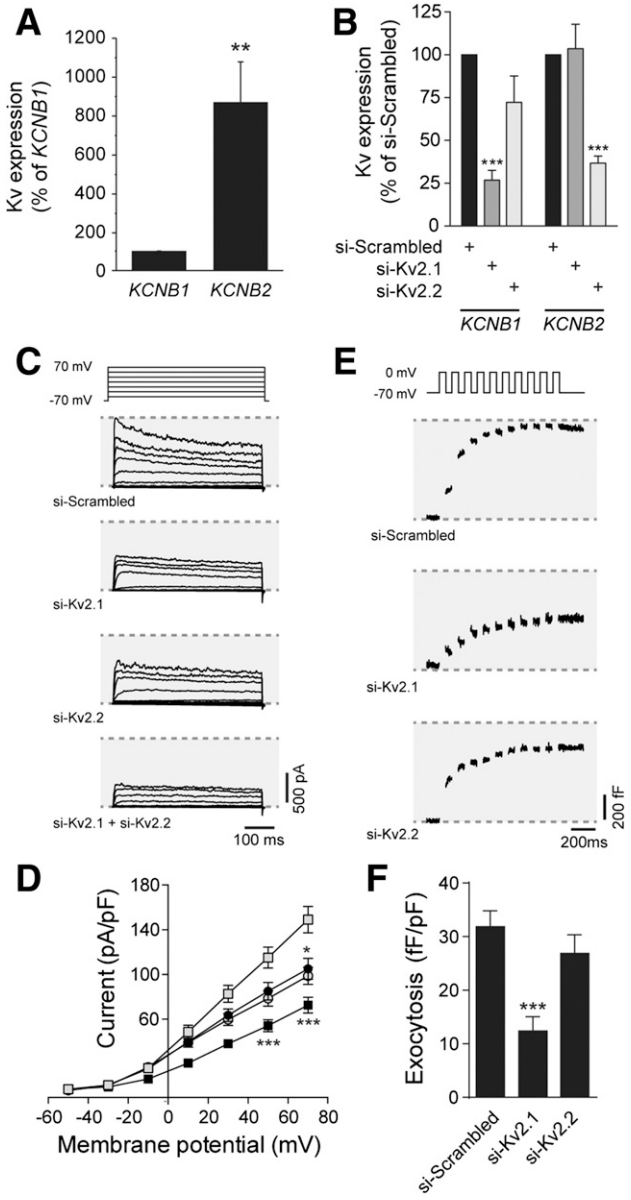

Figure 1—Kv2.1, but not Kv2.2, controls exocytosis in human β-cells. *A*: Expression of mRNA encoding Kv2.1 (*KCNB1*) and Kv2.2 (*KCNB2*) in islets from human donors assessed by quantitative PCR (n = 11 donors). *B*: Knockdown of *KCNB1* and *KCNB2* expression in human islet cells, assessed by quantitative PCR, following transfection with control siRNA duplexes (si-Scrambled) or siRNAs targeting Kv2.1 (si-Kv2.1) or Kv2.2 (si-Kv2.2) (n = 6 donors). Representative traces (*C*) and averaged current–voltage relationships (*D*) of Kv currents recorded from human β-cells following transfection with si-Scrambled (gray squares), si-Kv2.1 (black circles), si-Kv2.2 (gray circles), or both (black squares) (n = 20, 13, 21, and 17 cells from 4 donors, respectively). Representative capacitance traces (*E*) and averaged cumulative exocytotic responses (*F*) of human β-cells to a series of membrane depolarizations following transfection with si-Scrambled, si-Kv2.1, or si-Kv2.2 (n = 23, 32, and 31 cells from 5 donors, respectively). *P < 0.05; **P < 0.01; ***P < 0.001 compared with the Kv2.1 group (*A*) or scrambled control (*B–F*).

Kv2.1 Clusters in β-Cells

In human β-cells (Fig. 2*A*) and INS 832/13 cells (Fig. 2*B*) imaged by TIRF microscopy to visualize fluorescence within 100 nm above the coverslip, endogenous Kv2.1 is not homogenously distributed. Using an object-based colocalization routine considering centers within 0.3 μm as colocalized, a portion of these (25.6 ± 3.1% in human β-cells, n = 23 cells from three donors; 25.5 ± 2.4% in INS 832/13, n = 26 cells from three experiments) appear associated with an insulin granule. When expressed in INS 832/13 cells, mCherry-tagged WT Kv2.1 (mCherry-Kv2.1-WT) also forms membrane-localized clusters and can occasionally be seen to colocalize with secretory granules marked by NPY-Venus in fixed cells (Fig. 2*C*). Bleed-through of the Venus signal into the red channel does not account for the apparent colocalization (Supplementary Fig. 3).

Using a PAmCherry-tagged channel (PAmCherry-Kv2.1-WT), we performed PALM imaging and spatial pattern analysis (29) of Kv2.1 clusters in HEK 293 and INS 832/13 cells. In both cell types, PAmCherry-Kv2.1-WT was nonhomogenously distributed on the cell membrane (Fig. 3*A* and *B*), with 35–40% of tagged subunits being localized to clusters (Fig. 3*C*). Based on the average number of molecules per cluster (~25–40) (Fig. 3*D*) and assuming each tetrameric channel will have 3 to 4 detectable

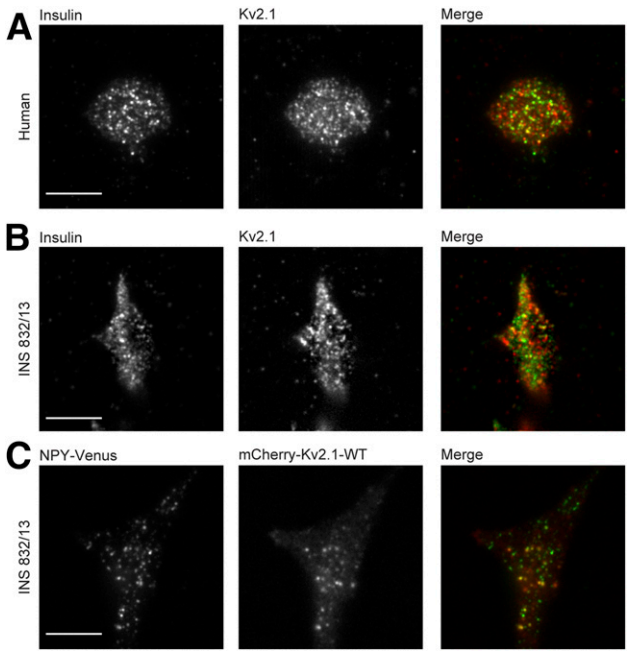

Figure 2—Kv2.1 forms clusters in insulin-secreting cells. Human β-cells (*A*) or INS 832/13 cells (*B*) were immunostained with anti-Kv2.1 (red) and anti-insulin (green) antibodies and visualized by TIRF microscopy (representative of 23 cells from 3 donors and 26 cells in 3 experiments, respectively). *C*: INS 832/13 cell expressing mCherry-Kv2.1-WT (red) and NPY-Venus (green; 33 cells in 3 experiments). Scale bars, 10 μm.

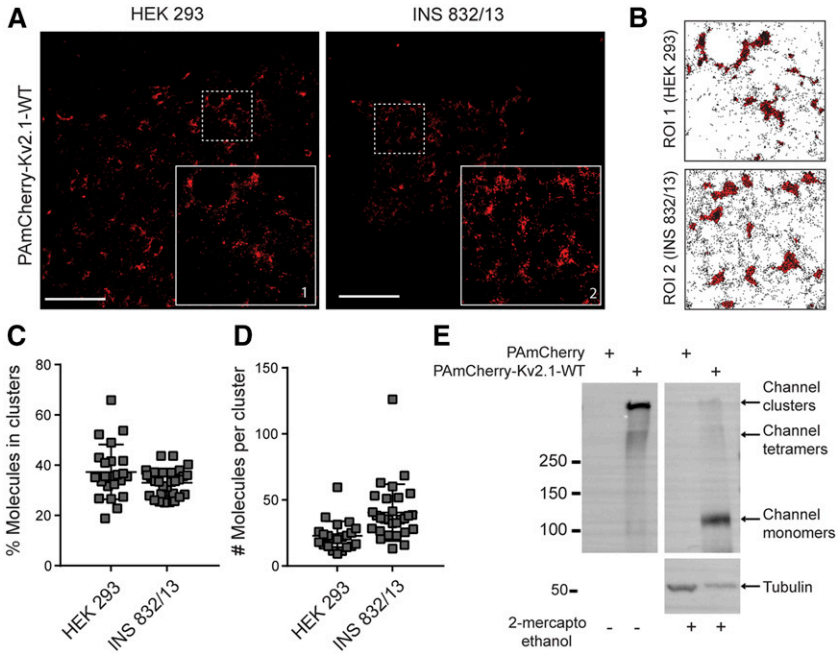

Figure 3—Superresolution imaging of Kv2.1 clusters. *A*: PALM images of HEK 293 and INS 832/13 cells expressing PAmCherry-Kv2.1-WT (red). Inset zoom-in area corresponds to the region of interest (ROI). Scale bars, 5 μm. *B*: PAmCherry-Kv2.1-WT molecule coordinate plots for ROIs in *A*, with cluster regions determined by spatial pattern analysis, highlighted in red in the background. The percentage of PAmCherry-Kv2.1-WT molecules found within clustered domains (*C*) and the average number of molecules per cluster (*D*) in HEK 293 cells ($n = 22$) and INS 832/13 cells ($n = 29$). *E*: Extracellular cross-linking with DTSSP followed by blotting of protein lysates with anti-Kv2.1 antibody demonstrates that the tagged (PAmCherry-Kv2.1-WT) channels form large-molecular-weight complexes at the cell surface, consistent with channel clustering. Breakdown of cross-links with 2-ME reveals the expression of channel monomers (representative of $n = 6$ experiments).

molecules, we estimate that Kv2.1 clusters contain 6–12 tetrameric channels on average. Extracellular cross-linking confirmed that these target to the plasma membrane, where they form large macromolecular complexes corresponding to multichannel clusters that barely migrate into the running gel (Fig. 3*E*). Following cleavage of the cross-link with 2-ME, these appear as single monomeric subunits.

Clustering of Kv2.1 Promotes Exocytosis

We generated clustering-deficient channels (mCherry-Kv2.1-ΔC318 and Myc-Kv2.1-ΔC318) (Fig. 4*A*), based on previous reports that a region in the C terminus is required for Kv2.1 clustering (13). These do not form clusters when expressed in HEK 293 cells (Fig. 4*B* and *D* and Supplementary Fig. 4) and form substantially fewer clusters in INS 832/13 cells (Fig. 4*C–F* and Supplementary Fig. 4). We found that the Kv2.1-ΔC318 constructs retained at least some ability to form clusters when in the INS 832/13 cells, which we attribute to an interaction with the endogenous full-length channel (Supplementary Fig. 5). Nonetheless, as demonstrated previously (13), the truncated channel formed many fewer membrane-resident clusters than the full-length channel despite similar levels of expression (2-ME–treated groups in Fig. 4*B* and *C*). Additionally, the density of membrane-resident secretory granules was reduced in INS 832/13 cells expressing mCherry-Kv2.1-ΔC318 compared with cells expressing mCherry-Kv2.1-WT (Fig. 4*E* and *F*), and colocalization was significantly reduced (from 29.1 ± 2.4 to 18.3 ± 1.8% of granules associated with an apparent Kv2.1 cluster; $n = 67, 69$ cells; $P < 0.001$), although this could result from reduced spot density, which was not corrected for.

Importantly, the truncated constructs retain similar electrical function to the WT channels in INS 832/13 (Fig. 5*A* and *B*) and HEK 293 (Supplementary Fig. 4*C*) cells, and both the Myc-Kv2.1-WT and Myc-Kv2.1-ΔC318 interacted equally with syntaxin 1A in INS 832/13 cells (Fig. 5*C* and *D*). However, although both the full-length mCherry-Kv2.1-WT and Myc-Kv2.1-WT enhanced depolarization-induced exocytosis in INS 832/13 cells, the clustering-deficient mutants did not (Fig. 5*E* and *F* and Supplementary Fig. 4*D*), suggesting that channel clustering per se, in addition to syntaxin 1A binding (7,12), is required to facilitate exocytosis.

Kv2.1 Clustering and Granule Recruitment to the Plasma Membrane

Knockdown of Kv2.1 (Fig. 6*A*) in INS 832/13 cells reduced the number of membrane-resident secretory granules at both low-glucose (1 mmol/L) and following 15- or 30-min stimulation with 16.7 mmol/L glucose (Fig. 6*B* and *C*). In cells expressing mCherry-Kv2.1-WT, glucose stimulation increased the density of membrane-resident secretory granules over 30 min, but this response was absent in cells expressing mCherry-Kv2.1-ΔC318 (Fig. 7*A–C*). Accordingly, expression of mCherry-Kv2.1-WT

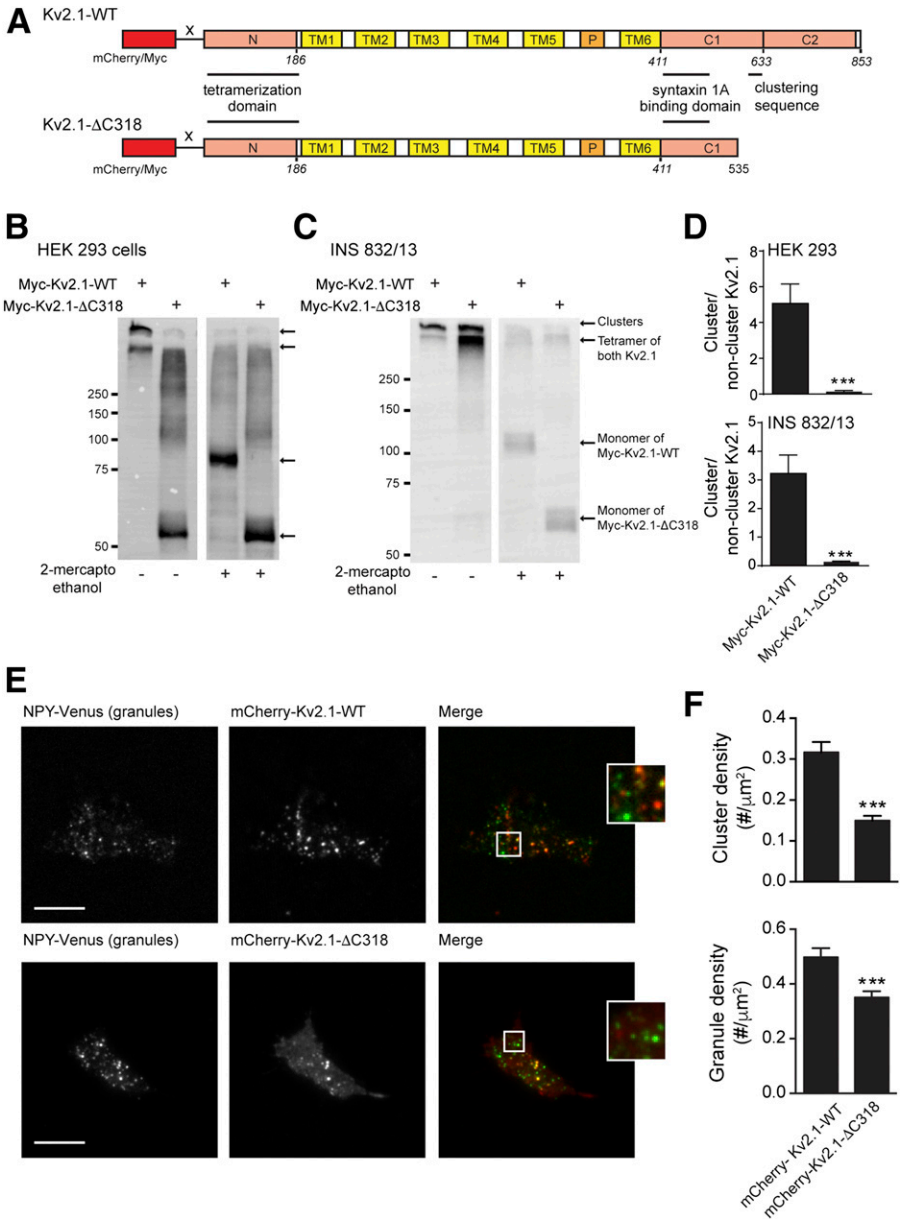

Figure 4—A clustering-deficient Kv2.1 reduces secretory granule recruitment to the plasma membrane. *A*: mCherry and Myc-tagged clustering-deficient Kv2.1 channels were generated by truncating the final 318 amino acids (mCherry/Myc-Kv2.1-ΔC318) of the rat sequence. *B–D*: When expressed in HEK 293 (*B*; n = 6 experiments) or INS 832/13 cells (*C*; n = 10 experiments), the Myc-Kv2.1-ΔC318 formed fewer high-molecular-weight clusters, which could be broken down to channel monomers by 2-ME. Although Myc-Kv2.1-ΔC318 retained some ability to form clusters in INS 832/13 cells, likely because of combination with native Kv2.1 (Supplementary Fig. 5), quantification (*D*; n = 6 and 10) revealed that the majority of the signal remains tetrameric (i.e., single-channel rather than cluster). Additional assessment of the clustering of these constructs is presented in Supplementary Fig. 4. *E* and *F*: When expressed in INS 832/13 cells and visualized by TIRF microscopy, mCherry-Kv2.1-ΔC318 forms fewer clusters than mCherry-Kv2.1-WT and results in fewer membrane-resident secretory granules, marked by NPY-Venus (n = 37; 62 cells from 5 experiments). Scale bars, 10 μm. ***$P < 0.001$ compared with mCherry-Kv2.1-WT.

also enhanced the glucose-dependent facilitation of exocytosis in INS 832/13 cells (Supplementary Fig. 6). Although glucose stimulation tended to increase the total mCherry-Kv2.1-WT cluster density (Fig. 7*C*), this was not statistically significant. Of note, we do not observe a glucose-dependent increase in Kv current in human β-cells (Supplementary Fig. 7).

Upregulation of Kv2.1 in T2D β-Cells Enhances Exocytosis and Insulin Secretion

Insulin secretion is impaired in T2D due at least in part to a reduced exocytotic response (33,34). A dissociation between secretory granules and sites of voltage-dependent Ca^{2+} entry has been reported in T2D models (35,36). In β-cells from donors with T2D, we find that Kv currents are similar

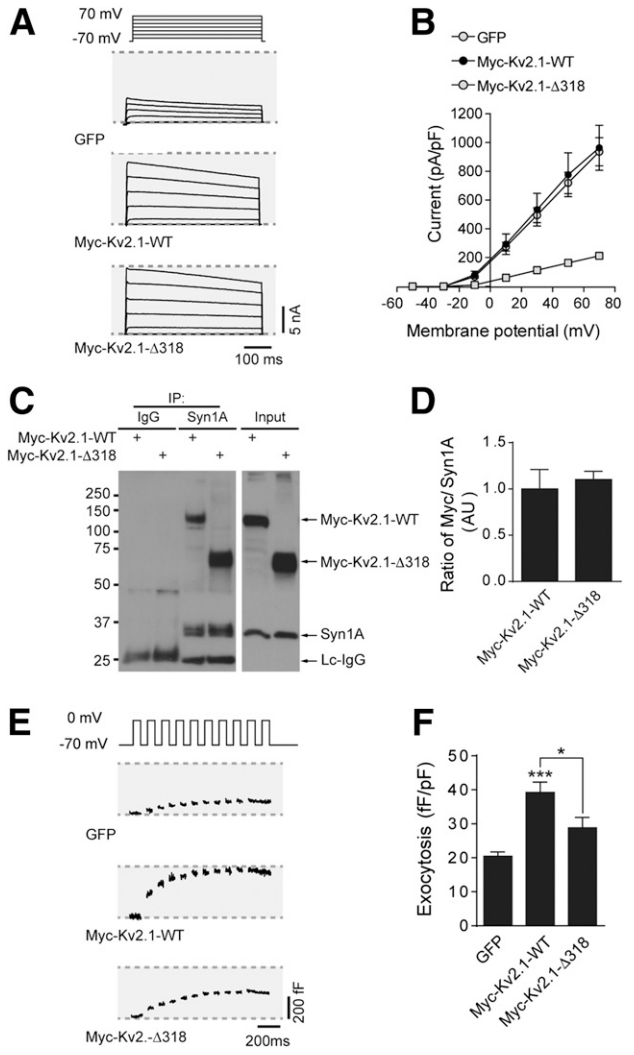

Figure 5—Clustering-deficient Kv2.1 retains electrical activity and syntaxin 1A binding, but does not facilitate exocytosis. Representative Kv currents (*A*) and quantified current-voltage relationships (*B*) from INS 832/13 cells expressing GFP alone, Myc-Kv2.1-WT, or Myc-Kv2.1-ΔC318 (n = 17, 19, and 18 cells, respectively). *C* and *D*: Coimmunoprecipitation (IP) of syntaxin 1A (Syn1A) pulled down both Myc-Kv2.1-WT and Myc-Kv2.1-ΔC318 equally well (n = 7 experiments). Representative capacitance traces (*E*) and cumulative exocytotic responses (*F*) of INS 832/13 cells expressing GFP alone, Myc-Kv2.1-WT, or Myc-Kv2.1-ΔC318 (n = 15, 22, and 17 cells, respectively). *P < 0.01 as indicated; ***P < 0.001 versus GFP control.

to those from ND donors (Fig. 8*A* and *B*), although knockdown of either *KCNB1* (Fig. 8*A*) or *KCNB2* (Fig. 8*B*) now fail to inhibit Kv currents. Indeed, compared with islets from ND donors, *KCNB1* (Fig. 8*C*) and *KCNB2* (data not shown) are lower in islets of donors with T2D (to 38 and 24% of control subjects, respectively). Consistent with our recent reports (33,37), we find that the ability of glucose to amplify β-cell exocytosis is impaired in T2D β-cells (Fig. 8*D* and *F*). Upregulation of Kv2.1-WT was sufficient to improve exocytotic function in β-cells from donors with T2D measured either by patch-clamp (Fig. 8*E* and *F*) or live-cell TIRF microscopy (Fig. 8*G–I*). Notably, live-cell TIRF imaging demonstrates that although the full-length Kv2.1-WT increases exocytosis in ND β-cells (Fig. 8*H* and *I*) and increases the exocytotic response in T2D β-cells to the level seen in control in ND cells (Fig. 8*H* and *J*), the truncated Kv2.1-ΔC318 construct is without effect. Finally, in islets from donors with T2D in which the insulin secretory response is impaired compared with matched ND control subjects (Supplementary Fig. 8), transduction with adenovirus expressing a full-length, but electrically inactive, Kv2.1 (Ad-Kv2.1$^{W365C/Y380T}$) increased glucose-stimulated insulin secretion (Fig. 8*J–L*).

DISCUSSION

The regulated exocytosis of insulin is disrupted in vitro, in animal models of T2D, and in β-cells from human donors with T2D (33,35,38,39). The mechanisms underlying this are not entirely clear, although reduced SNARE expression (40,41), altered granule-Ca^{2+} channel coupling (35,38), and impaired metabolic signaling (33) have all been suggested and point to an important role for dysregulation of the distal secretory machinery. In the current work, we present evidence suggesting that a reduction of Kv2.1 channels contributes to exocytotic dysfunction because these are required for efficient recruitment of secretory granules. Furthermore, clustering of the channels, in addition to syntaxin 1A binding (7,12), is required for glucose-dependent granule recruitment and the facilitation of exocytosis.

Kv2.1 is long known to contribute a majority of the delayed K^+ current in rodent (3,4) and human (3,31) β-cells. Although immunolocalization studies suggest that Kv2.2 is expressed in human δ-cells and regulates somatostatin secretion (8,9), these do not rule out expression in β-cells, as transcriptomic analysis (11) and experimental studies (10) suggest that Kv2.2 may be expressed at significant levels in these cells. Consistent with the latter reports, we observed higher expression of Kv2.2-encoding mRNA in human islets and INS 832/13 cells and found that this isoform mediates a substantial portion of the Kv current. However, Kv2.2 knockdown had no effect on β-cell exocytosis, consistent with its divergent C-terminal homology from Kv2.1 and its inability to bind the syntaxin 1A/SNAP-25 complex (32). However, given that the expression of *KCNB2* is reduced in T2D islets and upon metabolic perturbation in INS 832/13 cells (10), a role in insulin secretion cannot be ruled out.

In neurons, Kv2.1 channels localize to large plasma membrane clusters (42), the distribution of which is controlled by activity- (43) and cell cycle–dependent (44) (de)phosphorylation. An exact physiological role for Kv2.1 clusters is unclear, although they may be electrically silent (16) and act as platforms for channel insertion (18) at sites where the cortical endoplasmic reticulum interacts with the plasma membrane (19,45). Given the demonstration that Kv2.1 participates directly in exocytosis (7,12), we wondered whether this channel, like the L-type Ca^{2+} channel (46) with which it colocalizes (47), forms plasma membrane clusters in the β-cell. Indeed, native Kv2.1 in INS

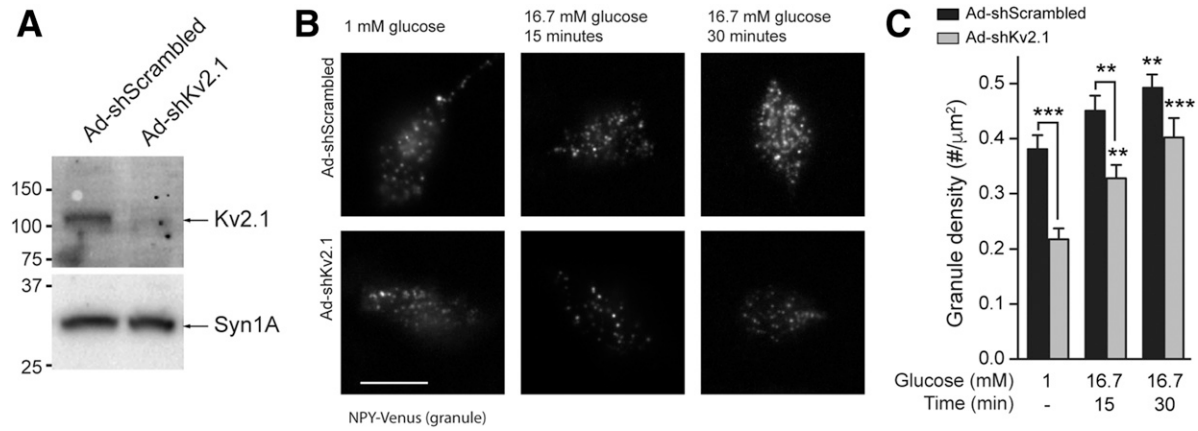

Figure 6—Kv2.1 and a role for the channel in granule recruitment. *A*: Knockdown of Kv2.1 protein in Ad-shKv2.1–infected INS 832/13 cells compared with control subjects (Ad-shScrambled; $n = 4$ experiments). *B* and *C*: Knockdown of Kv2.1 in INS 832/13 cells resulted in a decreased density of membrane-resident secretory granules marked with NPY-Venus and visualized by TIRF microscopy at both 1 and 16.7 mmol/L glucose. Representative images (*B*) and quantified data (*C*) are shown ($n = 30, 30, 27, 30, 28$, and 30 cells in 3 experiments). Syn1A, syntaxin 1A. Scale bar, 10 μm. $^{**}P < 0.01$; $^{***}P < 0.001$ compared with 1 mmol/L glucose control or as indicated.

832/13 cells and human β-cells form clusters at the plasma membrane as observed through both biochemical and imaging approaches. At least a subset of these clusters appear in close proximity to membrane-resident insulin granules and syntaxin 1A clusters; however, the exact relationship between granule docking/exocytosis sites and the Kv2.1 clusters remains to be resolved.

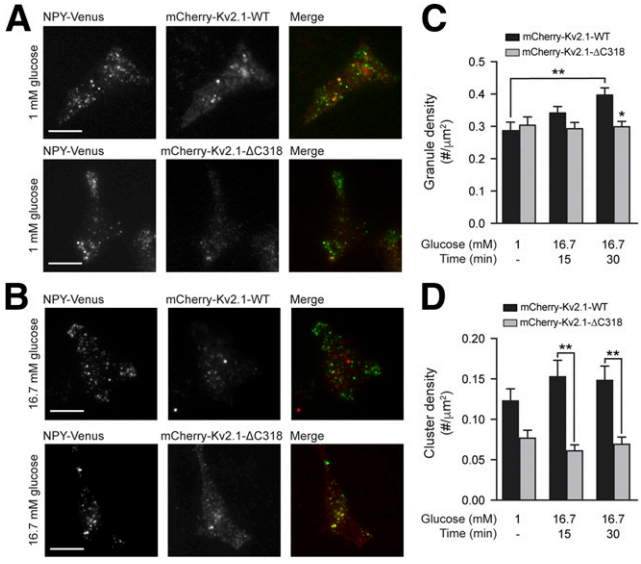

Figure 7—Kv2.1 clusters promote secretory granule recruitment. Representative images (*A* and *B*) and quantified data (*C* and *D*) of INS 832/13 cells expressing mCherry-Kv2.1-WT (red) or mCherry-Kv2.1-ΔC318 (red) and NPY-Venus (green) at 1 mmol/L glucose and after 15 or 30 min of 16.7 mmol/L glucose, visualized by TIRF microscopy. Glucose stimulation increased the density of membrane-resident secretory granules (*C*) in the mCherry-Kv2.1-WT group (black bars), but not the mCherry-Kv2.1-ΔC318 group (gray bars), the latter of which had fewer channel clusters (*D*). Scale bars, 10 μm. $^{*}P < 0.05$; $^{**}P < 0.01$ compared with the 1 mmol/L glucose condition, or as indicated.

Consistent with previous reports (13,15), the C terminus of the channel is required for clustering in HEK 293 cells. The ΔC318 C-terminal truncation did not, however, entirely abolish Kv2.1 clustering in INS 832/13 cells. This may result from heterotetramerization of the recombinant channel with native full-length Kv2.1 in these cells, although a role for localization to lipid rafts known to occur in β-cells (48) cannot be ruled out. Nonetheless, C terminus–mediated clustering of Kv2.1 tetramers is required for effective facilitation of insulin exocytosis in β-cells because the Kv2.1-ΔC318 is unable to facilitate exocytosis in INS 832/13 cells or human β-cells despite efficient syntaxin 1A binding, although altered interactions with other SNARE proteins cannot yet be ruled out. It should also be noted that the C-terminal truncation used here removes the distal C2 domain in addition to the clustering sequence (13). However, we have previously found no effect of the Kv2.1 C2 region on insulin exocytosis (7).

Declustering of Kv2.1 occurs during brain ischemia, which suggests the clusters may have an important pathophysiological role in neurons (49). In human β-cells, we show that *KCNB1* expression and the contribution of Kv2.1-mediated current is decreased in T2D. Consistent with an impact of this on insulin exocytosis, knockdown of *KCNB1* results in impaired secretory granule recruitment and exocytosis. Taken together, we hypothesize that a reduction of Kv2.1 expression contributes to the impairment of human β-cell exocytosis in T2D. The relationship of this to previous reports demonstrating reduced coupling between membrane-associated secretory granules, voltage-gated Ca^{2+} channels and sites of localized Ca^{2+} entry (35,38) in models of T2D remains unclear. It is unlikely that reduced Kv2.1 expression is entirely responsible for impaired β-cell function in T2D, and indeed, secretory granule fusion in T2D β-cells expressing the full-length Kv2.1 remained somewhat lower than ND β-cells overexpressing

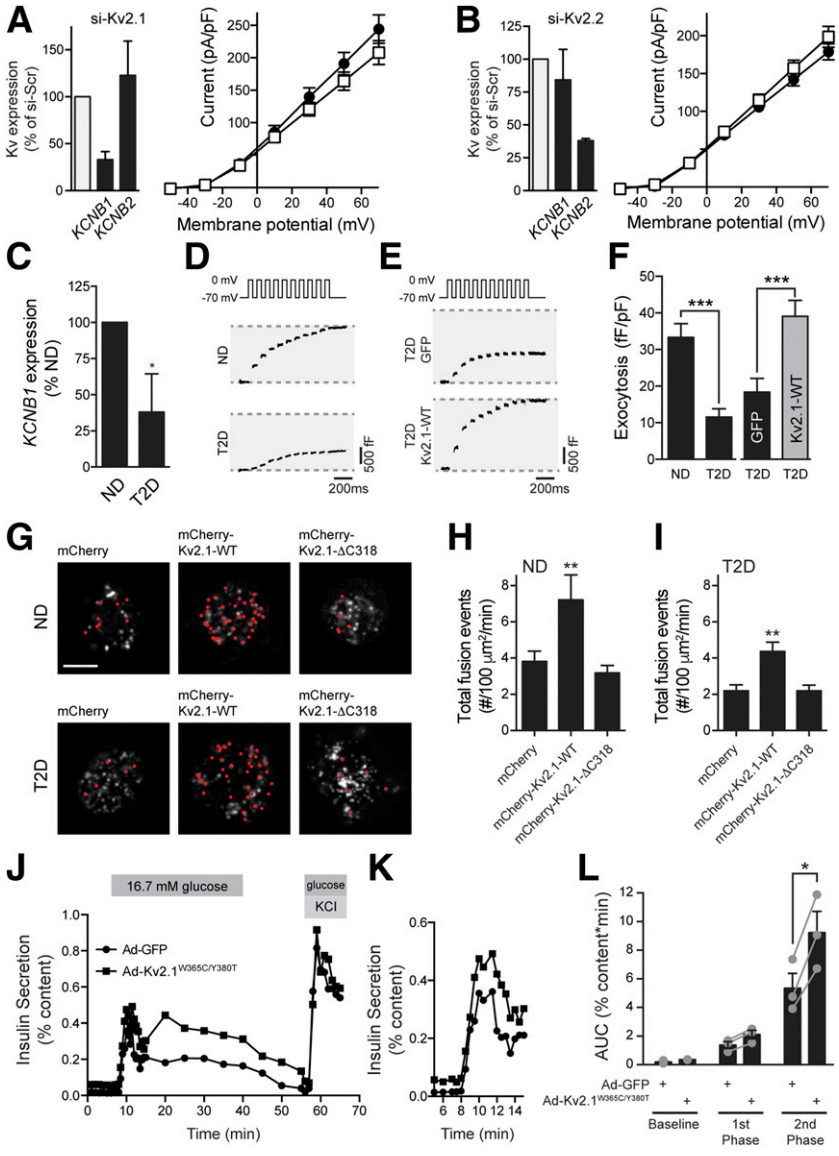

Figure 8—Upregulation of Kv2.1 in human T2D β-cells improves exocytotic function. Knockdown of Kv2.1 (*A*; *KCNB1*; n = 13 and 13 cells from 2 donors) or Kv2.2 (*B*; *KCNB2*; n = 19 and 23 cells from 3 donors) expression failed to reduce voltage-dependent K^+ currents in β-cells from donors with T2D. *C*: Expression of Kv2.1 (*KCNB1*) mRNA in islets from ND donors or donors with T2D (n = 11 and 5 donors, respectively). Representative capacitance responses at 10 mmol/L glucose from untransfected (*D*) β-cells of ND donors and donors with T2D and of transfected β-cells (*E*) of donors with T2D expressing GFP alone or together with Kv2.1-WT. *F*: The cumulative exocytotic responses from *D* and *E* (n = 30 cells from 3 ND donors and n = 30, 32 and 34 cells from 3–5 donors with T2D). *G*: Images from live-cell TIRF of ND and T2D β-cells expressing mCherry, mCherry-Kv2.1-WT, or mCherry-Kv2.1-ΔC318 and the granule marker NPY-EGFP (greyscale). Red dots indicate exocytotic events occurring over 2 min upon increasing glucose from 2.8 to 5 mmol/L. Scale bars, 5 μm. Average frequency of exocytotic events in ND (*H*; n = 17, 20, and 21 cells from 2 donors) and T2D (*I*; n = 24, 34, and 30 cells from 2 donors with T2D) β-cells. *J* and *K*: Insulin secretory profiles of islets from a donor with T2D transduced with control adenovirus (Ad-GFP; circles) or an electrically silent full-length Kv2.1 (Ad-Kv2.1$^{W365C/Y380T}$; squares). The first phase secretory response is shown on expanded time scale (*K*) (one donor; experiment run in duplicate). *L*: Averaged and individual (circles) area under the curve (AUC) values for baseline, first-phase, and second-phase responses of islets from donors with T2D transduced as in *J* and *K* (n = 3 donors in duplicate). *P < 0.05 versus ND or as indicated; **P < 0.01 versus mCherry; ***P < 0.001 as indicated.

this construct. However, it seems possible that Kv2.1 channel clusters contribute to an excitosome complex thought to be important for coordinating signaling, excitability and Ca^{2+} influx at the exocytotic site (50,51). Disruption of Kv2.1 clustering likely results in dysregulation of key interactions at these sites required for efficient secretory granule docking and exocytosis. It should also be considered that Kv2.1 clusters might play more than a simply structural role at the exocytotic site, because channels within clusters are capable of sensing membrane voltage and producing gating currents (16) and of interacting with the ER to potentially regulate intracellular Ca^{2+} stores (19).

Plasma membrane protein clustering is emerging as an important level of organization, primed to facilitate

cellular functions (52), including insulin secretion (53). Our data provide evidence that Kv2.1 clusters play a key role in facilitating insulin exocytosis and implicate an important pathophysiological contribution of the loss of Kv2.1 in T2D. The regulation of Kv2.1 clusters in concert with many other protein-protein interactions at the plasma membrane might be important for the efficient recruitment, docking, and priming of secretory granules.

Acknowledgments. The authors thank the Human Organ Procurement and Exchange (HOPE) and Trillium Gift of Life Network (TGLN) programs for their efforts in procuring pancreas for research. The authors also thank Dr. James Shapiro (Department of Surgery, University of Alberta, Edmonton, Alberta, Canada), Dr. Tatsuya Kin (Clinical Islet Laboratory, University of Alberta), and Mr. James Lyon (Alberta Diabetes Institute IsletCore, University of Alberta) for work isolating human research islets and Dr. Michael Tamkun (Colorado State University, Fort Collins, CO) for helpful discussion.

Funding. Human research islet isolations were supported by the Alberta Diabetes Foundation and the University of Alberta. Research was funded by operating grants from the Canadian Institutes of Health Research (MOP310536 to P.E.M. and MOP93659 to N.T.), the Natural Sciences and Engineering Research Council (NSERC-DG327988 to N.T.), and the National Institutes of Health (DK-46492 to C.B.N.). Infrastructure funding was in part from the Canada Foundation for Innovation (IOF17625 to N.T.). J.F. was supported by studentships from the Alberta Diabetes Institute and the University of Alberta. J.M.G. was supported by the International Research Training Group in Membrane Biology (NSERC-CREATE-414205-2012). N.T. holds an Alberta Innovates Health Solutions Research Scholarship. P.E.M. is supported by a 2016–2017 Killam Professorship.

Duality of Interest. No potential conflicts of interest relevant to this article were reported.

Author Contributions. J.F., X.D., G.P., K.S., A.B., J.M.G., L.S., D.G.-A., J.E.M.F., and H.Y.G. performed experiments and analyzed data. K.S., M.J., D.G.-A., H.Y.G., and C.B.N. generated key reagents. J.F., X.D., J.M.G., M.J., J.E.M.F., C.B.N., N.T., and P.E.M. designed experiments and analyzed data. J.F. and P.E.M. wrote the manuscript. All of the authors reviewed, edited, and approved the final version of the manuscript. P.E.M. is the guarantor of this work and, as such, had full access to all the data in the study and takes responsibility for the integrity of the data and the accuracy of the data analysis.

Prior Presentation. Parts of this study were presented in abstract form at the 77th Scientific Sessions of the American Diabetes Association, San Diego, CA, 9–13 June 2017.

References

1. Kahn SE, Cooper ME, Del Prato S. Pathophysiology and treatment of type 2 diabetes: perspectives on the past, present, and future. Lancet 2014;383:1068–1083
2. Rorsman P, Braun M. Regulation of insulin secretion in human pancreatic islets. Annu Rev Physiol 2013;75:155–179
3. MacDonald PE, Sewing S, Wang J, et al. Inhibition of Kv2.1 voltage-dependent K+ channels in pancreatic beta-cells enhances glucose-dependent insulin secretion. J Biol Chem 2002;277:44938–44945
4. Jacobson DA, Kuznetsov A, Lopez JP, Kash S, Ammälä CE, Philipson LH. Kv2.1 ablation alters glucose-induced islet electrical activity, enhancing insulin secretion. Cell Metab 2007;6:229–235
5. Herrington J, Sanchez M, Wunderler D, et al. Biophysical and pharmacological properties of the voltage-gated potassium current of human pancreatic beta-cells. J Physiol 2005;567:159–175
6. Braun M, Ramracheya R, Bengtsson M, et al. Voltage-gated ion channels in human pancreatic beta-cells: electrophysiological characterization and role in insulin secretion. Diabetes 2008;57:1618–1628
7. Dai XQ, Manning Fox JE, Chikvashvili D, et al. The voltage-dependent potassium channel subunit Kv2.1 regulates insulin secretion from rodent and human islets independently of its electrical function. Diabetologia 2012;55:1709–1720
8. Yan L, Figueroa DJ, Austin CP, et al. Expression of voltage-gated potassium channels in human and rhesus pancreatic islets. Diabetes 2004;53:597–607
9. Li XN, Herrington J, Petrov A, et al. The role of voltage-gated potassium channels Kv2.1 and Kv2.2 in the regulation of insulin and somatostatin release from pancreatic islets. J Pharmacol Exp Ther 2013;344:407–416
10. Jensen MV, Haldeman JM, Zhang H, et al. Control of Kv2.2 expression by pyruvate-isocitrate cycling regulates glucose-stimulated insulin secretion. J Biol Chem 2013;288:23128–23140
11. Blodgett DM, Nowosielska A, Afik S, et al. Novel observations from next-generation RNA sequencing of highly purified human adult and fetal islet cell subsets. Diabetes 2015;64:3172–3181
12. Singer-Lahat D, Sheinin A, Chikvashvili D, et al. K+ channel facilitation of exocytosis by dynamic interaction with syntaxin. J Neurosci 2007;27:1651–1658
13. Lim ST, Antonucci DE, Scannevin RH, Trimmer JS. A novel targeting signal for proximal clustering of the Kv2.1 K+ channel in hippocampal neurons. Neuron 2000;25:385–397
14. Tamkun MM, O'connell KMS, Rolig AS. A cytoskeletal-based perimeter fence selectively corrals a sub-population of cell surface Kv2.1 channels. J Cell Sci 2007;120:2413–2423
15. Baver SB, O'Connell KMS. The C-terminus of neuronal Kv2.1 channels is required for channel localization and targeting but not for NMDA-receptor-mediated regulation of channel function. Neuroscience 2012;217:56–66
16. O'Connell KMS, Loftus R, Tamkun MM. Localization-dependent activity of the Kv2.1 delayed-rectifier K+ channel. Proc Natl Acad Sci U S A 2010;107:12351–12356
17. Fox PD, Loftus RJ, Tamkun MM. Regulation of Kv2.1 K(+) conductance by cell surface channel density. J Neurosci 2013;33:1259–1270
18. Deutsch E, Weigel AV, Akin EJ, et al. Kv2.1 cell surface clusters are insertion platforms for ion channel delivery to the plasma membrane. Mol Biol Cell 2012;23:2917–2929
19. Fox PD, Haberkorn CJ, Weigel AV, et al. Plasma membrane domains enriched in cortical endoplasmic reticulum function as membrane protein trafficking hubs. Mol Biol Cell 2013;24:2703–2713
20. Hohmeier HE, Newgard CB. Cell lines derived from pancreatic islets. Mol Cell Endocrinol 2004;228:121–128
21. Lyon J, Manning Fox JE, Spigelman AF, et al. Research-focused isolation of human islets from donors with and without diabetes at the Alberta Diabetes Institute IsletCore. Endocrinology 2016;157:560–569
22. Dundr M, Ospina JK, Sung M-H, et al. Actin-dependent intranuclear repositioning of an active gene locus in vivo. J Cell Biol 2007;179:1095–1103
23. Subach FV, Patterson GH, Manley S, Gillette JM, Lippincott-Schwartz J, Verkhusha VV. Photoactivatable mCherry for high-resolution two-color fluorescence microscopy. Nat Methods 2009;6:153–159
24. Yuan T, Lu J, Zhang J, Zhang Y, Chen L. Spatiotemporal detection and analysis of exocytosis reveal fusion "hotspots" organized by the cytoskeleton in endocrine cells. Biophys J 2015;108:251–260
25. Betzig E, Patterson GH, Sougrat R, et al. Imaging intracellular fluorescent proteins at nanometer resolution. Science 2006;313:1642–1645
26. Githaka JM, Vega AR, Baird MA, Davidson MW, Jaqaman K, Touret N. Ligand-induced growth and compaction of CD36 nanoclusters enriched in Fyn induces Fyn signaling. J Cell Sci 2016;129:4175–4189
27. Jaqaman K, Loerke D, Mettlen M, et al. Robust single-particle tracking in live-cell time-lapse sequences. Nat Methods 2008;5:695–702
28. Thomann D, Rines DR, Sorger PK, Danuser G. Automatic fluorescent tag detection in 3D with super-resolution: application to the analysis of chromosome movement. J Microsc 2002;208:49–64
29. Williamson DJ, Owen DM, Rossy J, et al. Pre-existing clusters of the adaptor Lat do not participate in early T cell signaling events. Nat Immunol 2011;12:655–662

30. Motulsky HJ, Brown RE. Detecting outliers when fitting data with nonlinear regression - a new method based on robust nonlinear regression and the false discovery rate. BMC Bioinformatics 2006;7:123

31. MacDonald PE, Ha XF, Wang J, et al. Members of the Kv1 and Kv2 voltage-dependent K(+) channel families regulate insulin secretion. Mol Endocrinol 2001;15: 1423–1435

32. Wolf-Goldberg T, Michaelevski I, Sheu L, Gaisano HY, Chikvashvili D, Lotan I. Target soluble N-ethylmaleimide-sensitive factor attachment protein receptors (t-SNAREs) differently regulate activation and inactivation gating of Kv2.2 and Kv2.1: Implications on pancreatic islet cell Kv channels. Mol Pharmacol 2006;70: 818–828

33. Ferdaoussi M, Dai X, Jensen MV, et al. Isocitrate-to-SENP1 signaling amplifies insulin secretion and rescues dysfunctional β cells. J Clin Invest 2015;125:3847–3860

34. Qin T, Liang T, Zhu D, et al. Munc18b increases insulin granule fusion, restoring deficient insulin secretion in type-2 diabetes human and Goto-Kakizaki rat islets with improvement in glucose homeostasis. EBioMedicine 2017;16:262–274

35. Hoppa MB, Collins S, Ramracheya R, et al. Chronic palmitate exposure inhibits insulin secretion by dissociation of Ca(2+) channels from secretory granules. Cell Metab 2009;10:455–465

36. Collins SC, Hoppa MB, Walker JN, et al. Progression of diet-induced diabetes in C57BL6J mice involves functional dissociation of Ca2(+) channels from secretory vesicles. Diabetes 2010;59:1192–1201

37. Gooding JR, Jensen MV, Dai X, et al. Adenylosuccinate is an insulin secretagogue derived from glucose-induced purine metabolism. Cell Reports 2015;13: 157–167

38. Collins SC, Salehi A, Eliasson L, Olofsson CS, Rorsman P. Long-term exposure of mouse pancreatic islets to oleate or palmitate results in reduced glucose-induced somatostatin and oversecretion of glucagon. Diabetologia 2008;51:1689–1693

39. Rosengren AH, Braun M, Mahdi T, et al. Reduced insulin exocytosis in human pancreatic β-cells with gene variants linked to type 2 diabetes. Diabetes 2012;61: 1726–1733

40. Ostenson C-G, Gaisano H, Sheu L, Tibell A, Bartfai T. Impaired gene and protein expression of exocytotic soluble N-ethylmaleimide attachment protein receptor complex proteins in pancreatic islets of type 2 diabetic patients. Diabetes 2006;55: 435–440

41. Andersson SA, Olsson AH, Esguerra JLS, et al. Reduced insulin secretion correlates with decreased expression of exocytotic genes in pancreatic islets from patients with type 2 diabetes. Mol Cell Endocrinol 2012;364:36–45

42. Trimmer JS. Immunological identification and characterization of a delayed rectifier K+ channel polypeptide in rat brain. Proc Natl Acad Sci U S A 1991;88: 10764–10768

43. Cerda O, Trimmer JS. Activity-dependent phosphorylation of neuronal Kv2.1 potassium channels by CDK5. J Biol Chem 2011;286:28738–28748

44. Cobb MM, Austin DC, Sack JT, Trimmer JS. Cell cycle-dependent changes in localization and phosphorylation of the plasma membrane Kv2.1 K+ channel impact endoplasmic reticulum membrane contact sites in COS-1 cells. J Biol Chem 2015; 290:29189–29201

45. Du J, Tao-Cheng JH, Zerfas P, McBain CJ. The K+ channel, Kv2.1, is apposed to astrocytic processes and is associated with inhibitory postsynaptic membranes in hippocampal and cortical principal neurons and inhibitory interneurons. Neuroscience 1998;84:37–48

46. Bokvist K, Eliasson L, Ammälä C, Renström E, Rorsman P. Co-localization of L-type Ca2+ channels and insulin-containing secretory granules and its significance for the initiation of exocytosis in mouse pancreatic B-cells. EMBO J 1995;14:50–57

47. Fox PD, Haberkorn CJ, Akin EJ, Seel PJ, Krapf D, Tamkun MM. Induction of stable ER-plasma-membrane junctions by Kv2.1 potassium channels. J Cell Sci 2015;128:2096–2105

48. Xia F, Gao X, Kwan E, Lam PPL, Chan L, Sy K, et al Disruption of pancreatic beta-cell lipid rafts modifies Kv2.1 channel gating and insulin exocytosis. J Biol Chem 2004;279:24685–24691

49. Misonou H, Mohapatra DP, Menegola M, Trimmer JS. Calcium- and metabolic state-dependent modulation of the voltage-dependent Kv2.1 channel regulates neuronal excitability in response to ischemia. J Neurosci 2005;25: 11184–11193

50. MacDonald PE. Signal integration at the level of ion channel and exocytotic function in pancreatic β-cells. Am J Physiol Endocrinol Metab 2011;301:E1065–E1069

51. Leung YM, Kwan EP, Ng B, Kang Y, Gaisano HY. SNAREing voltage-gated K+ and ATP-sensitive K+ channels: tuning beta-cell excitability with syntaxin-1A and other exocytotic proteins. Endocr Rev 2007;28:653–663

52. Garcia-Parajo MF, Cambi A, Torreno-Pina JA, Thompson N, Jacobson K. Nanoclustering as a dominant feature of plasma membrane organization. J Cell Sci 2014;127:4995–5005

53. Gandasi NR, Barg S. Contact-induced clustering of syntaxin and munc18 docks secretory granules at the exocytosis site. Nat Commun 2014; 5:3914